



Thrombospondin 1 is associated with MASH and hepatic macrophage inflammatory responses via CD47

Qiling Liu^{1,2,#}, Chenmin Fan^{1,3,#}, Binger Xu^{1,4,#}, Xinyu Yang¹, Xiaoyang Sun¹, Yuying Zhang¹, Shuqi Li¹, Miao Zhang¹, Xilei Ban¹, Guligeina Aikebaier¹, Ziping Bai¹, Wenfei Duan¹, Yang He¹, Hongmei Yan¹, Xinxia Chang¹, Mingfeng Xia^{1,5}, Xiaopeng Zhu¹ , Xin Gao¹ , Hua Bian¹ 

Keywords:

Metabolic dysfunction-associated steatotic liver disease, metabolic dysfunction-associated steatohepatitis, thrombospondin 1, CD47, M1 macrophage

Citation: Liu Q, Fan C, Xu B, Yang X, Sun X, Zhang Y, Li S, Zhang M, Ban X, Aikebaier G, Bai Z, Duan W, He Y, Yan H, Chang X, Xia M, Zhu X, Gao X, Bian H.

Thrombospondin 1 is associated with MASH and hepatic macrophage inflammatory responses via CD47. *Metab Target Organ Damage*. 2026;6:25. <https://dx.doi.org/10.20517/mtod.2026.11>

Received: 11 Jan 2026

First Decision: 18 Mar 2026

Revised: 14 May 2026

Accepted: 18 May 2026

Published: 3 Jun 2026

Academic Editor:

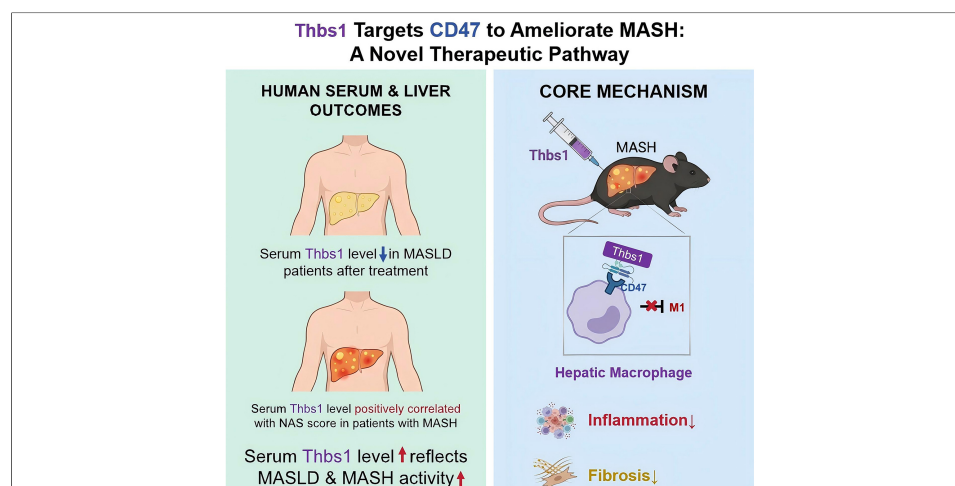
Amedeo Lonardo

Copy Editor:

Ting-Ting Hu

Production Editor:

Ting-Ting Hu



Abstract

Aim: To investigate the effects and potential mechanisms of thrombospondin 1 (Thbs1) in metabolic dysfunction-associated steatohepatitis (MASH).

Methods: Serum Thbs1 concentrations were quantified in patients with metabolic dysfunction-associated steatotic liver disease (MASLD) before and after intervention, and in a biopsy-proven cohort. Moreover, a diet-induced MASH mouse model was established using a Western diet and fructose water. The involvement of CD47 was evaluated in mice with liver-specific CD47 overexpression. Further, the immunomodulatory effects of Thbs1 were assessed in lipopolysaccharide-treated RAW264.7 macrophages.

Results: Serum Thbs1 levels significantly decreased in patients with MASLD after treatment. Additionally, patients with MASH exhibited higher Thbs1 levels than non-MASH individuals. This elevated Thbs1 level was modestly associated with histopathological severity. Furthermore, short-term Thbs1 administration was associated with reduced hepatic inflammation and early fibrotic features, accompanied by decreased hepatic

¹Department of Endocrinology and Metabolism, Zhongshan Hospital, Fudan Institute for Metabolic Diseases, Fudan University, Shanghai 200032, China.

²Department of Hematology, The First Medical Centre, Chinese PLA General Hospital, Beijing 100039, China.

³Department of Cardiology, Heart Center of Fujian Province, Fujian Medical University Union Hospital, Fuzhou 350001, Fujian, China.

⁴Department of Endocrinology, Shanghai Public Health Clinical Center, Shanghai 201508, China.

⁵Department of Endocrinology and Metabolism, Wusong Branch of Zhongshan Hospital, Fudan University, Shanghai 200940, China.

[#]These authors contributed equally to this work.

Correspondence to: Dr. Xiaopeng Zhu, Dr. Xin Gao, Dr. Hua Bian, Department of Endocrinology and Metabolism, Zhongshan Hospital, Fudan Institute for Metabolic Diseases, Fudan University, Shanghai 200032, China. E-mail: zhu.xiaopeng@zs-hospital.sh.cn; zhongshan_endo@126.com; bian.hua@zs-hospital.sh.cn

macrophage infiltration and M1 macrophage-associated signatures in MASH mice. However, liver-specific CD47 overexpression attenuated the observed effects of Thbs1. *In vitro*, Thbs1 reduced lipopolysaccharide-induced M1 macrophage-associated signatures and pro-inflammatory cytokine expression.

Conclusion: Thbs1 suppresses M1 macrophage-associated signatures via CD47 signaling, thereby attenuating liver inflammation and early fibrotic features in MASH mice. These data highlight the Thbs1-CD47 axis as a potential stage-informed target for MASH treatment.

INTRODUCTION

Metabolic dysfunction-associated steatotic liver disease (MASLD), previously known as non-alcoholic fatty liver disease (NAFLD), is the most prevalent chronic liver disorder globally^[1]. It is a multisystem disorder characterized by hepatic steatosis accompanied by insulin resistance and metabolic dysfunction^[2]. Metabolic dysfunction-associated steatohepatitis (MASH) represents a severe MASLD subtype associated with increased risks of systemic metabolic complications and adverse hepatic outcomes. Approximately 15% of patients with MASH develop cirrhosis, advanced fibrosis, or hepatocellular carcinoma within 10-15 years after diagnosis, and thus the disease constitutes a major public health concern^[3]. However, the cellular and molecular mechanisms underlying MASH remain unclear, and effective pharmacotherapies are lacking.

Thrombospondin-1 (Thbs1) is a secreted matricellular protein with multiple structural domains that interact with diverse receptors to modulate processes such as immune regulation, angiogenesis, cell adhesion, and apoptosis^[4]. Thbs1 expression is upregulated in cirrhotic livers from patients with MASH and in MASH mouse models, plausibly reflecting its roles in lipid metabolism and insulin resistance^[5,6]. Thbs1 suppresses fatty acid uptake through CD36, reducing hepatic *de novo* lipogenesis and intracellular triglyceride (TG) accumulation to improve steatosis^[7]. Thbs1 also influences hepatic inflammation and immune responses: it can dampen macrophage inflammatory activation by promoting anti-inflammatory cytokines and suppressing pro-inflammatory cytokines and T-cell activation^[8]. However, although Thbs1 treatment alleviates hepatic steatosis in diet-induced MASLD, its role in MASH remains unclear^[7].

Cluster of differentiation 47 (CD47) is a transmembrane protein widely expressed across cell types and serves as a receptor for Thbs1. Cell-based studies showed that Thbs1 binding to CD47 disrupts CD47-CD14 coupling, thereby limiting TLR-dependent signal 1 (NF- κ B/AP-1 priming), downregulating pro-interleukin (IL)-1 β and pro-caspase-1 in macrophages, and modulating inflammasome-mediated IL-1 β maturation^[8]. These findings support a net anti-inflammatory role for Thbs1-CD47 in macrophages. Nevertheless, the specific mechanisms, context-dependence, and *in vivo* relevance of the Thbs1-CD47 pathway in MASH remain unclear.

To address these gaps, we aimed to: (1) determine the association between serum Thbs1 and MASH severity in humans; (2) evaluate the therapeutic efficacy of Thbs1 in a diet-induced MASH mouse model; and (3) delineate the contribution of CD47 to Thbs1's effects, focusing on hepatic macrophage inflammatory responses. These objectives collectively interrogate the Thbs1-CD47 axis in the context of MASH.

METHODS

Randomized, parallel-controlled, open-label, multicenter clinical trial in MASLD (NCT00633282)

We analyzed data from a previously reported multicenter, randomized, parallel-controlled, open-label clinical trial (Trial Registration: ClinicalTrials.gov, NCT00633282. Registered on 3rd March 2008, <https://clinicaltrials.gov/study/NCT00633282>)^[9]. Briefly, 184 patients with MASLD across three centers with liver fat content (LFC) > 13% by proton magnetic resonance spectroscopy (¹H-MRS) were randomized to receive 16 weeks of lifestyle intervention (LSI), LSI plus pioglitazone (PGZ), or LSI plus berberine (BBR). LFC changes were measured by ¹H-MRS. Serum samples were collected at baseline and after treatment, stored at -80 °C, and assayed for Thbs1 by enzyme-linked immunosorbent assay (ELISA).

Cohort of patients with pathological results from liver biopsy

A cohort of 191 patients who underwent ultrasound-guided liver biopsy was established in the Department of Endocrinology and Metabolism at Zhongshan Hospital, Fudan University. These biopsies were conducted in patients aged 18-75 years who presented with indications for liver biopsy between 2012 and 2019. Data on relevant clinical parameters, including age, sex, and body mass index (BMI), were collected. Fasting serum was obtained from blood collected from these patients and kept at -80 °C for subsequent analyses. Patients were excluded from the study if they were diagnosed with hepatitis B, hepatitis C, or any other liver diseases; had known acute or chronic severe illnesses or organ dysfunction (excluding obesity or type 2 diabetes); exhibited excessive alcohol consumption (> 140 g/week for men and > 70 g/week for women); or were using liver-protective agents or hepatotoxic medications^[10]. Liver tissue samples were obtained through ultrasound-guided liver biopsy and evaluated by clinical pathologists blinded to clinical data. The severity of the liver lesions was assessed using the NAFLD Activity Score (NAS) proposed by the NASH Clinical Research Network Pathology Committee. MASH was diagnosed based on the concurrent presence of steatosis, ballooning degeneration, and lobular inflammation^[11]. The patients were categorized into two groups according to their pathological outcomes: MASH ($n = 152$) and non-MASH ($n = 39$). Serum Thbs1 concentrations were measured using ELISA. The study complied with the Declaration of Helsinki and was approved by the Ethics Committee of Zhongshan Hospital, Fudan University (Approval No. B2022-152). All participants provided written informed consent.

Reagents and antibodies

The recombinant Thbs1 protein (CU45) was purchased from Novoprotein (Shanghai, China). CD47 antibody (66304-1-Ig) was obtained from Proteintech (USA). Stearoyl-CoA desaturase-1 antibody (2438S), fatty acid synthase (FASN) antibody (3180S), horseradish peroxidase (HRP)-linked anti-mouse IgG (7076S), and HRP-linked anti-rabbit IgG (7074S) were purchased from Cell Signaling (USA). Sterol regulatory element-binding protein-1c (SREBP-1c) antibody (sc-365513) was obtained from Santa Cruz, USA. Glyceraldehyde-3-phosphate dehydrogenase (GAPDH) antibody (EPR16891) and α -tubulin antibody (ab7291) were purchased from Abcam (Cambridge, UK).

Animal experiments

Male C57BL/6J mice (GemPharmatech Co., Ltd., China) were maintained under institutional animal care guidelines (Institute for Nutritional Sciences). Eight-week-old mice were fed either chow (P1101F, SLAC, China) or a Western diet (TD120528, SYSE Bio-tech Co., Ltd., China) plus 42 g/L D(-)-fructose in drinking water (ST2312, Beyotime, China) for up to 24 weeks. At week 22, mice were randomly assigned to different experimental groups: CD47 overexpression (OE) group, received a single tail-vein injection of liver-specific CD47 OE adenovirus (2×10^9 PFU/mouse; in 200 μ L PBS) and control groups, received control adenovirus. Adenoviruses were from GeneChem Co., Ltd. (China). Mice were monitored for adverse events by researchers who were blinded to the group assignments. Forty-eight hours post-adenovirus injection, mice with Western diet and fructose solution-induced MASH were assigned into three experimental groups: a

control virus and control solution group (vehicle + PBS), control virus and Thbs1 group (vehicle + Thbs1), and liver-specific CD47 OE adenovirus and Thbs1 group (CD47 OE + Thbs1). The vehicle + Thbs1 and CD47 OE + Thbs1 groups received daily subcutaneous Thbs1 (0.5 mg/kg) for 10 days, while vehicle + PBS controls received PBS. The injection volume was 2 μ L per gram of body weight. Serum TG, total cholesterol (TC), alanine aminotransferase (ALT), and aspartate aminotransferase (AST) were measured using commercial assay kits (Nanjing Jiancheng Bioengineering Institute, China). All animal experimental protocols were approved by the Animal Welfare and Ethics Committee of the Department of Laboratory Animal Science, Fudan University (Approval No. 202111017S).

Liver histological analysis

Mouse liver tissues were fixed in paraformaldehyde, dehydrated using a series of ethanol and xylene solutions, and embedded in paraffin. Paraffin sections were mounted onto slides for staining following the protocols of the hematoxylin and eosin (H&E) staining kit (Wuhan Servicebio Technology Co., Ltd., China) and Picro Sirius Red Stain kit (Shanghai MaoKang Biotechnology Co., Ltd., China). The severity of liver lesions was assessed using the NAS. MASH was diagnosed when pathological examination of the liver revealed concurrent steatosis, ballooning degeneration, and lobular inflammation^[11].

Liver immunohistochemistry and immunofluorescence analysis

Liver tissue macrophage immunohistochemical staining and immunofluorescence detection were performed using rat anti-F4/80 (Wuhan Servicebio Technology Co., Ltd., China) as previously reported^[12,13].

Intraperitoneal glucose tolerance test (IPGTT) and intraperitoneal insulin tolerance test (IPITT)

IPGTT was conducted a day after completion of the Thbs1 treatment, while IPITT was performed three days after IPGTT. The tests were performed as described previously^[14].

Cell culture and treatment

Mouse RAW264.7 cells were cultured in DMEM (Gibco, USA) containing 4.5 g/L glucose, 10% fetal bovine serum (Gibco, USA), and 1% penicillin/streptomycin (Gibco, USA). Upon reaching approximately 50% confluence, the cells were treated with either 10 μ g/mL Thbs1 protein or PBS control. Following a 2-h incubation period, cells were treated with 100 ng/mL lipopolysaccharide (LPS) (Sigma-Aldrich) for 24 h.

Quantitative real-time polymerase chain reaction (qRT-PCR)

RNAiso Plus (Takara, Japan) was used to extract total RNA from the liver or treated cells according to the manufacturer's instructions. Reverse transcription was performed using the PrimeScript FAST RT Reagent Kit with gDNA Eraser (Takara, Japan) to obtain cDNA samples. The cDNA was subsequently diluted to an appropriate concentration and analyzed by qRT-PCR using Hieff qPCR SYBR Green Master Mix (Yeasen, China) according to the manufacturer's protocol on a Roche Applied Science LightCycler 480. Different housekeeping genes were used as internal references according to sample type: *Actb* (Gene ID: 11461) was used as the internal reference gene for mouse liver tissues, while *Rplp0* (Gene ID: 11837) was used for treated RAW264.7 cells. The relative mRNA expression levels of target genes were calculated using the $2^{-\Delta\Delta C_t}$ method. Primers used for qRT-PCR were specifically designed for mouse (*Mus musculus*) sequences, and their specificity was verified by BLAST alignment and melting curve analysis. [Supplementary Table 1](#) lists the primer sequences used in this study.

Western blot

Proteins from the liver tissues of mice were extracted using RIPA lysis buffer containing protease and phosphatase inhibitors. Proteins were quantified using the BCA protein assay kit (Beyotime, China). Protein samples (20 μ g) were loaded onto SDS-PAGE gels (Epizyme Biotech Co., Ltd., Shanghai, China) and

transferred to polyvinylidene difluoride (PVDF) membranes (Millipore, USA). The PVDF membranes were blocked with 5% skim milk at 20–25 °C for 1–2 h, followed by overnight incubation with primary antibodies at 4 °C. After thorough washing, the membranes were incubated with the corresponding secondary antibodies in 5% skim milk at room temperature for 1–2 h, followed by another thorough wash. Finally, a Western blot Enhanced chemiluminescence substrate kit (Millipore, USA) was used for imaging. Densitometric quantification was performed using ImageJ software 1.46r (ImageJ, USA).

Statistical analysis

For patients with MASLD enrolled in the randomized controlled trial (RCT), paired *t*-tests or Wilcoxon signed-rank tests were used to compare serum Thbs1 levels and other parameters before and after treatment depending on the normality of the data. For patients in the liver biopsy cohort, unpaired *t*-tests or Mann-Whitney tests were employed to compare serum Thbs1 levels and other parameters between non-MASH and MASH groups, based on the normality of the data. To account for the ordinal nature of the NAS, Spearman's rank correlation analysis was utilized to evaluate the correlation between serum Thbs1 levels and NAS. Multivariate regression analyses based on multiple imputed datasets were performed to assess the association between Thbs1 and histological disease severity after adjusting for potential confounders. Linear regression models were applied to evaluate the association between Thbs1 and NAS, adjusting for age, sex, BMI, liver enzymes, glucose metabolism, lipid profiles, and fibrosis stage. Results are presented as β coefficients with 95% confidence intervals (CIs). All statistical analyses for animal and cell experiments (including those in [Supplementary Figures 1–3](#)) were performed as follows: unpaired *t*-tests were used to compare statistical significance between two groups, whereas one-way analysis of variance (ANOVA) followed by Tukey's multiple comparisons test was used to evaluate statistical significance between more than two groups. Two-tailed $P < 0.05$ was considered statistically significant. Where applicable, statistical outliers were identified and excluded from analysis using the ROUT method ($Q = 5\%$). Statistical analyses were performed using GraphPad Prism 10.5.0 (GraphPad Software Inc., USA).

RESULTS

Serum Thbs1 levels correlate with MASH severity

In the RCT cohort (NCT00633282), 16 weeks of LSI and/or pharmacotherapy (PGZ or BBR) reduced LFC, IL-6, ALT, and BMI in patients with MASLD, accompanied by a significant decline in serum Thbs1 [[Figure 1A–D](#), [Supplementary Figure 1A](#) and [B](#)]. These data suggest an association between Thbs1 and MASLD severity. To further explore the possible association between Thbs1 and MASH, we measured serum Thbs1 concentrations in a cohort of 191 patients with liver biopsy-confirmed pathological diagnoses. Patients with simultaneous hepatic steatosis, ballooning degeneration, and lobular inflammation were categorized into the MASH group ($n = 152$), and the remaining patients were assigned to the non-MASH group ($n = 39$). Notably, patients in the MASH group demonstrated significantly elevated levels of serum Thbs1, ALT, and AST as well as elevated BMI compared with those in the non-MASH group [[Figure 1E](#), [Supplementary Figure 1C–E](#)]. In this liver biopsy cohort, we observed a statistically significant, albeit modest, positive correlation between serum Thbs1 concentration and NAS ($r = 0.1839$, $P = 0.0106$, [Figure 1F](#)), suggesting a modest association between serum Thbs1 levels and histological severity of MASH. To address potential confounding and further evaluate these associations, we performed multivariable analysis adjusting for key clinical covariates, such as BMI, ALT, AST, age, sex, diabetes mellitus, fasting plasma glucose, TG, TC, high-density lipoprotein (HDL) cholesterol, low-density lipoprotein (LDL) cholesterol, and fibrosis stage. Multivariate linear regression demonstrated that Thbs1 maintained its association with NAS ($\beta = 0.048$, 95%CI: 0.010–0.087, $P = 0.013$; [Supplementary Table 2](#)). Although established factors, such as BMI and fibrosis stage, showed stronger associations with NAS, Thbs1 maintained its association after full adjustment. These findings indicate that serum Thbs1 is associated with histological severity in MASH [[Figure 1G](#)].

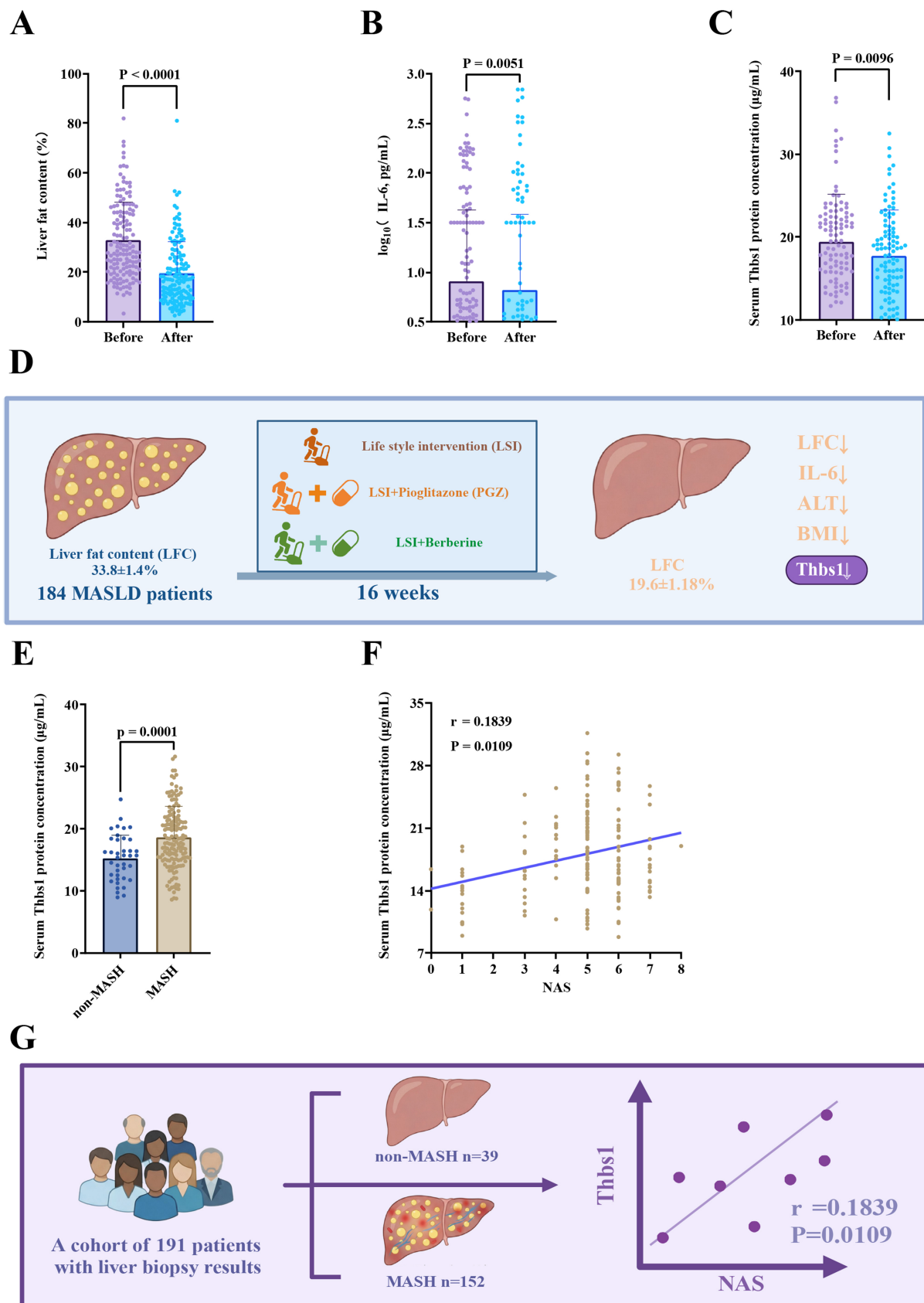


Figure 1. Serum Thbs1 correlates with MASH severity. (A-D) In MASLD patients (RCT, $n = 184$), 16 weeks of LSI and/or PGZ/BBR reduced LFC, IL-6, ALT, BMI, and serum Thbs1; (E) Patients with MASH showed significantly higher serum Thbs1 levels than those in the non-MASH group; (F) Serum Thbs1 levels showed a modest positive correlation with NAS ($r = 0.1839$, $P = 0.0106$). The solid line represents the linear regression fit for visual illustration of the trend; (G) Schematic representation of serum Thbs1 dynamics in MASLD/MASH. Data are presented as mean \pm SD. P values are indicated in figures. Statistical analyses were performed using unpaired t -tests or Mann-Whitney tests for group comparisons, and Spearman's correlation analysis for association studies, as appropriate. $P <$

0.05 was considered statistically significant. ALT: Alanine aminotransferase; BBR: berberine; BMI: body mass index; IL-6: interleukin-6; LFC: liver fat content; LSI: lifestyle intervention; MASLD: metabolic dysfunction-associated steatotic liver disease; MASH: metabolic dysfunction-associated steatohepatitis; NAS: NAFLD activity score; PGZ: pioglitazone; RCT: randomized controlled trial; SD: standard deviation; Thbs1: thrombospondin-1.

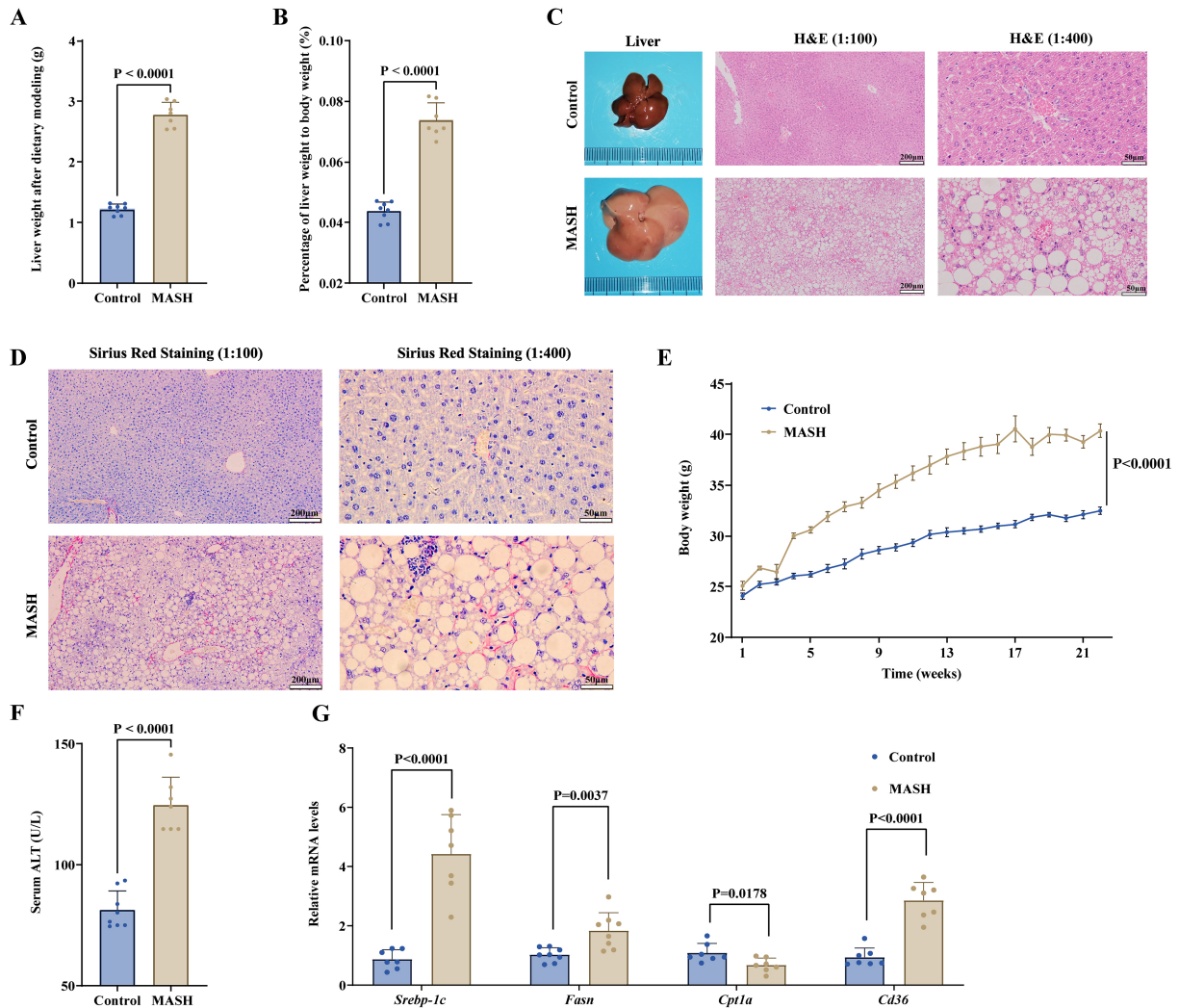


Figure 2. Long-term administration of a Western diet and fructose solution to mice induces a MASH model. (A and B) Increased liver weight and liver:body weight ratio in MASH; (C and D) Representative gross liver morphology, H&E staining (scale bars = 200 μ m for 1:100 and 50 μ m for 1:400), and Sirius Red staining (scale bars = 200 μ m for 1:100 and 50 μ m for 1:400) of both the control and MASH groups; (E) The body weight trends of the control and MASH groups were monitored over a period of 22 weeks; (F) The mice in the MASH group exhibited notably elevated serum ALT levels in comparison to those in the control group; (G) Comparative analysis of the relative expression levels of lipid synthesis- and metabolism-related mRNAs between the control and the MASH groups. Data are presented as mean \pm SD. Statistical significance was evaluated using two-tailed Student's *t*-test. $P < 0.05$ was considered statistically significant. For animal experiments, $n = 8$ mice per group were initially included; after outlier exclusion using ROUT ($Q = 5\%$), 7-8 samples per group were used for statistical analysis. ALT: Alanine aminotransferase; H&E: hematoxylin and eosin; MASH: metabolic dysfunction-associated steatohepatitis; mRNA: messenger RNA; ROUT: robust regression and outlier removal; SD: standard deviation; *Srebp-1c*: sterol regulatory element-binding protein-1c; *Fasn*: fatty acid synthase; *Cpt1a*: carnitine palmitoyltransferase 1a; *Cd36*: cluster of differentiation 36.

Long-term administration of a Western diet and fructose solution to mice induces MASH

To assess the efficacy of Thbs1, we created a diet-induced MASH animal model. Following a 22-week feeding period, mice fed a Western diet and fructose solution (MASH) exhibited a significant increase in liver weight and liver:body weight ratio when compared to those in mice receiving standard chow diet (control) [Figure 2A and B]. The livers of mice from the MASH group exhibited an enlarged, whitish appearance with

rounded edges and worse histopathology, accompanied by severe hepatic steatosis, lobular inflammation, and hepatocyte ballooning [Figure 2C]. Sirius Red collagen staining of the livers demonstrated normal findings in the control group, whereas MASH mice exhibited expanded portal area staining, increased interstitial collagen deposition, and fibrosis scores ranging from F1 to F2 [Figure 2D]. Additionally, MASH mice demonstrated a significant increase in overall body weight by the end of the feeding period [Figure 2E]. Serum analysis showed significantly elevated ALT, TG, and TC levels in MASH mice compared with those in controls [Figure 2F, Supplementary Figure 2C and D]. Although serum AST levels did not show a statistically significant increase, ALT is a more sensitive and specific marker for early hepatocyte injury in murine models of MASH. MASH mice showed upregulation of genes associated with *de novo* lipogenesis (*Srebp-1c* and *Fasn*) and fatty acid uptake (*Cd36*) and downregulation of lipid oxidation-related genes (*Cpt1a*) compared to the controls [Figure 2G]. In conclusion, a MASH mouse model was successfully established through a 22-week feeding regimen consisting of a Western diet and fructose solution.

Short-term administration of Thbs1 significantly improves liver inflammation and fibrosis in mice with diet-induced MASH

Given the strong correlation observed between serum Thbs1 levels and MASLD progression, particularly in terms of MASH severity, we hypothesized that Thbs1 may have therapeutic potential for treating MASH. To validate this hypothesis and explore the underlying mechanisms, we randomly assigned mice with MASH into three experimental groups at the 22nd week of the Western diet and fructose solution feeding regimen [Figure 3A]. Successful hepatic CD47 OE was confirmed via protein expression analysis [Figure 3B and C]. Subsequently, phenotypic analysis was performed [Figure 3D and E, Supplementary Figure 3A-C], which revealed no statistically significant differences in body weight, liver weight, or fat mass between the vehicle + PBS and vehicle + Thbs1 groups. This observation can be explained by the comparatively short span of the 10-day treatment period compared with the overall course of MASH. Likewise, intervention with Thbs1 did not notably enhance glucose tolerance or attenuate insulin resistance in MASH mice [Supplementary Figure 3D and E]. Although there were no significant changes in serum AST levels [Supplementary Figure 3F], Thbs1 intervention significantly reduced serum TC and TG levels [Supplementary Figure 3G and H], possibly because of its ability to decrease hepatic *de novo* lipogenesis. Histopathological analysis revealed that despite the absence of significant differences in hepatic steatosis between the vehicle + PBS and vehicle + Thbs1 groups, the administration of Thbs1 resulted in a notable decrease in lobular inflammation, reduction in inflammatory infiltration, and attenuation of early fibrotic features [Figure 3F].

At the protein expression level, Thbs1 administration did not significantly alter the expression of hepatic *de novo* lipogenesis-related proteins [Supplementary Figure 3I-L], consistent with the histopathological observations. Regarding the gene expression of inflammatory cytokines in the liver, the administration of Thbs1 markedly decreased the levels of *Il-1b* and *Il-12a* [Figure 3G], further validating the ability of Thbs1 to attenuate inflammation. Additionally, hepatic mRNA expression of fibrosis markers, including *Ccn2*, *Tgfb1*, *Col1a1*, *Col1a2*, and *Acta2*, was reduced following intervention with Thbs1 [Figure 3H]. This suggests that Thbs1 can reduce the progression of early fibrotic features in MASH. In conclusion, short-term subcutaneous administration of Thbs1 significantly attenuated liver inflammation and early fibrotic features in MASH mice.

Liver-specific CD47 OE antagonizes the therapeutic effects of Thbs1 on MASH

The mechanisms underlying the modulatory effects of Thbs1 on MASH remain unclear. CD47 interacts with its ligand Thbs1 to participate in immunoregulation. Therefore, we hypothesized that Thbs1 exerts modulatory effects on MASH by modulating inflammatory responses through CD47. Using the animal models established herein, we further analyzed phenotypic differences between the vehicle + Thbs1 and CD47 OE + Thbs1 groups. Compared with mice in the vehicle + Thbs1 group, mice in the CD47 OE + Thbs1

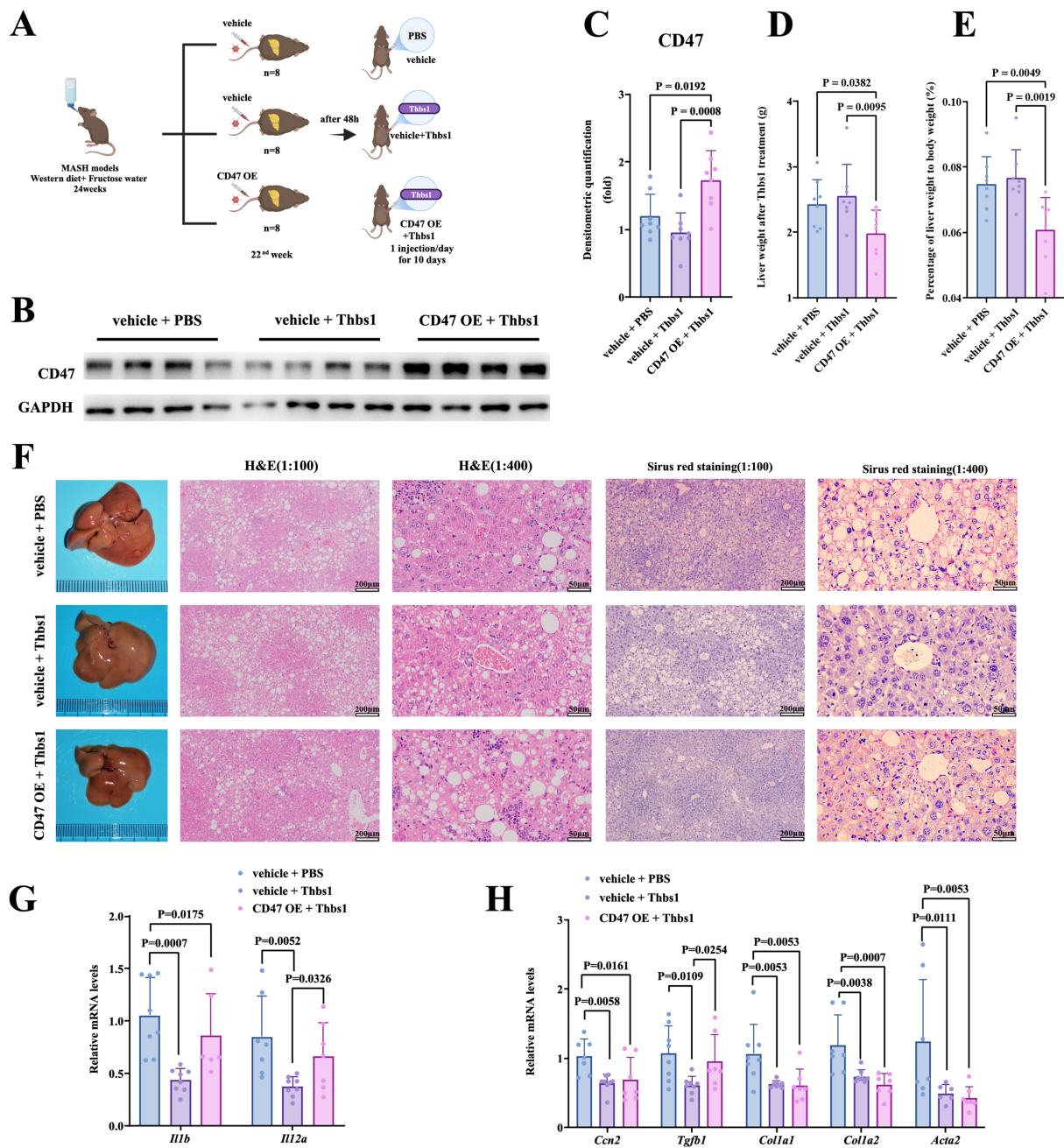


Figure 3. Liver-specific CD47 OE attenuated the effects of Thbs1 in diet-induced MASH mice. (A) Experimental design to verify the modulatory effects of Thbs1 and its correlation with CD47; (B and C) Western blot and quantification of CD47 OE; (D and E) Post-intervention liver weight and liver:body weight ratio across groups; (F) Representative gross liver morphology, H&E staining (scale bars = 200 μ m for 1:100 and 50 μ m for 1:400), and Sirius Red staining (scale bars = 200 μ m for 1:100 and 50 μ m for 1:400); (G and H) Post-intervention hepatic mRNA expression of inflammatory factors (*Il-1b*, *Il-12 α* , and *Cd14*) and fibrosis markers (*Ccn2*, *Tgfb1*, *Colla1*, *Colla2*, and *Acta2*). Data are presented as mean \pm SD. For *in vivo* experiments, $n = 8$ mice per group were initially included; after outlier exclusion using ROUT ($Q = 5\%$), 6-8 samples per group were used for statistical analysis. Statistical differences among multiple groups were analyzed using one-way ANOVA followed by Tukey's multiple comparisons test. $P < 0.05$ was considered statistically significant. ANOVA: Analysis of variance; CD47: cluster of differentiation 47; H&E: hematoxylin and eosin; MASH: metabolic dysfunction-associated steatohepatitis; mRNA: messenger RNA; OE: overexpression; ROUT: robust regression and outlier removal; SD: standard deviation; Thbs1: thrombospondin-1; *Il1 β* : interleukin-1 β ; *Il12 α* : interleukin-12 α ; *Ccn2*: cellular communication network factor 2; *Tgfb1*: transforming growth factor- β 1; *Colla1*: collagen type I alpha 1 chain; *Colla2*: collagen type I alpha 2 chain; *Acta2*: actin alpha 2.

group exhibited a significant reduction in liver weight and liver:body weight ratio [Figure 3D and E]. However, there were no statistically significant differences in body weight, fat mass, serum AST levels, TC, or TG between the two groups [Supplementary Figure 3A-C and F-H]. Additionally, the CD47 OE + Thbs1

group exhibited lower blood glucose levels 15 and 30 min after insulin injection [Supplementary Figure 3E]. This phenomenon may be attributed to diminished insulin tolerance, which was possibly induced by the high degree of liver inflammation and early fibrotic features. Histopathological analysis indicated that OE of CD47 in the liver counteracted the modulatory effects of Thbs1, which featured significantly increased lobular inflammatory infiltration, more pronounced interstitial collagen deposition and liver fibrosis, and similar lipid deposition [Figure 3F].

At the protein expression level, liver-specific OE of CD47 did not significantly alter hepatic lipogenic protein expression [Supplementary Figure 3I-L]. However, OE of CD47 in the liver significantly diminished the effect of Thbs1 in attenuating inflammation and early fibrotic features [Figure 3G and H]. Notably, Thbs1 significantly reduced hepatic *Cd14* mRNA expression, whereas CD47 OE robustly reversed this reduction. In conclusion, although short-term subcutaneous intervention with Thbs1 significantly attenuated liver inflammation and early fibrotic features in mice with MASH, these modulatory effects were inhibited by liver-specific OE of CD47.

Thbs1 suppresses M1 macrophage-associated signatures to attenuate MASH via CD47

To elucidate the specific molecular mechanisms by which Thbs1 improves MASH through CD47, we further analyzed the molecular phenotypes of mouse livers. Notable variations were observed in the hepatic mRNA expression levels of the macrophage marker *Cd68* as well as the pro-inflammatory M1 macrophage markers *Cd86* and *Nos2* among the three groups [Figure 4A], suggesting that Thbs1 and CD47 may influence MASH by modulating hepatic macrophages. We performed F4/80 immunohistochemistry and immunofluorescence staining to assess macrophage infiltration in the liver [Figure 4B]. Qualitative evaluation of representative images suggested that compared to the vehicle + PBS group, the vehicle + Thbs1 group demonstrated a marked decrease in the staining area of macrophages. Conversely, the CD47 OE + Thbs1 group exhibited an apparent increase in macrophage-stained regions, characterized by larger lipid vacuoles, compared with those in the vehicle + Thbs1 group. Notably, macrophages in the CD47 OE + Thbs1 group displayed a dense and clustered distribution pattern, suggesting a more severe degree of infiltration and inflammatory activity. The immunofluorescence findings were in agreement with the immunohistochemical observations, further supporting these qualitative interpretations.

The recruitment and inflammatory activation of hepatic mononuclear macrophages constitute pivotal mechanisms in the development of MASH. Kupffer cells, liver-resident macrophages, and monocytes recruited by inflammatory factors secreted by activated Kupffer cells into the liver can differentiate into pro-inflammatory M1 macrophages. These pro-inflammatory macrophages exacerbate hepatic inflammation and promote liver fibrosis by secreting signaling molecules, such as TGF β 1, to activate hepatic stellate cells, ultimately leading to MASH progression^[15]. Consequently, we hypothesized that Thbs1 may exert modulatory effects on MASH by acting through CD47 to regulate macrophage immune responses and inhibit the differentiation of macrophages into the inflammatory M1 phenotype. To verify this hypothesis, we established an *in vitro* model using RAW264.7 cells. The model was subsequently divided into three distinct groups: control group (PBS treatment only), LPS group (PBS treatment and LPS stimulation), and Thbs1 + LPS group (Thbs1 treatment and LPS stimulation) [Figure 4C]. The results indicated that Thbs1 markedly inhibited LPS-induced mRNA expression of M1 macrophage markers (*Adgre1* and *Cd86*) and concurrently enhanced the mRNA expression of the M2 macrophage marker (*Arg1*) [Figure 4D]. Simultaneously, Thbs1 significantly inhibited the mRNA expression of pro-inflammatory cytokines secreted by M1 macrophages (*Il-6*, *Il-1b*, *Tnf*, *Il-23a*, and *Ccl2*) and promoted the mRNA expression of anti-inflammatory cytokines secreted by M2 macrophages (*Il-10*) [Figure 4E]. In conclusion, Thbs1 can inhibit M1 macrophage-associated signatures via CD47, thereby modulating the inflammatory responses of liver macrophages and consequently attenuating inflammation and early fibrotic features in MASH.

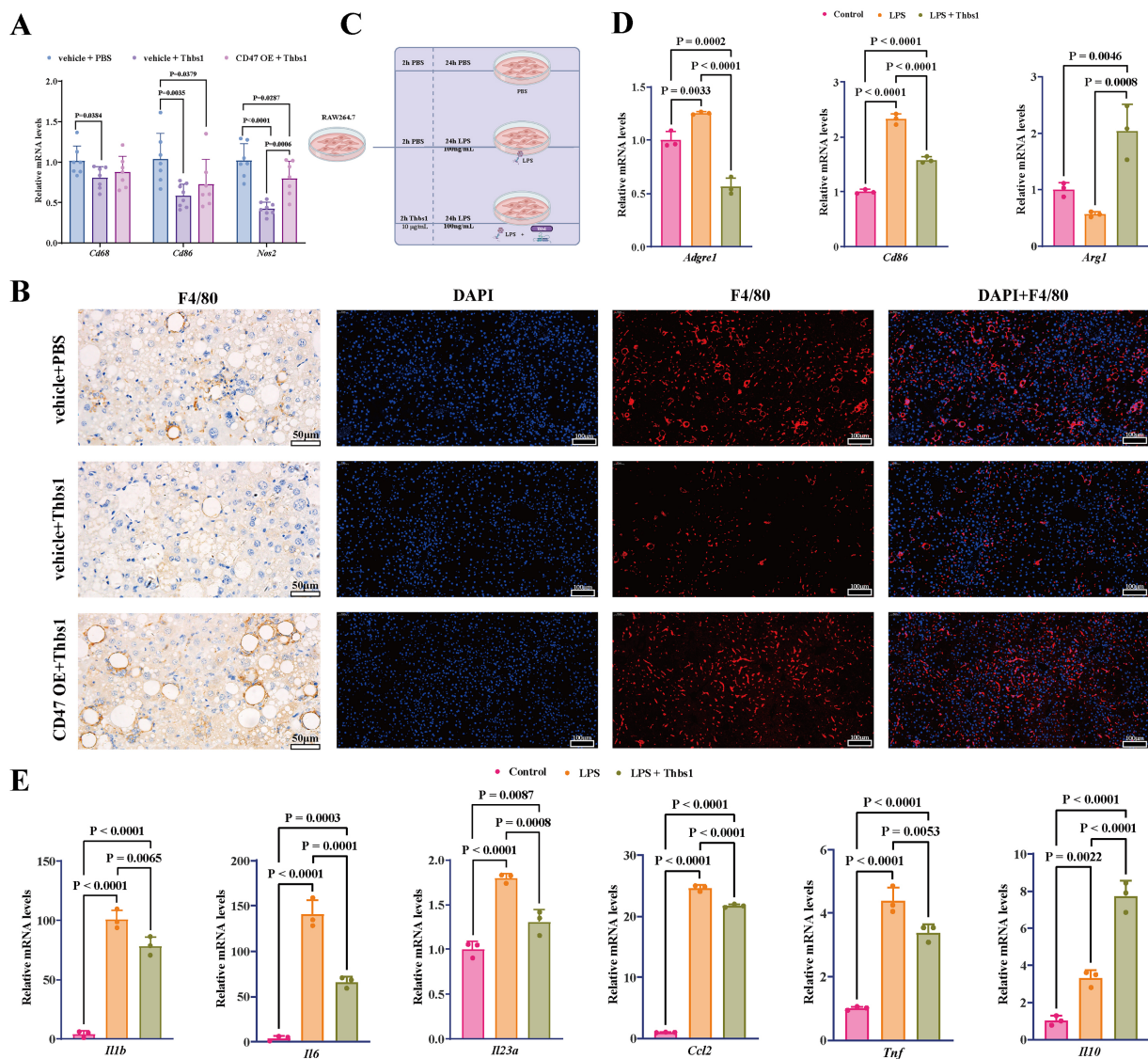


Figure 4. Thbs1 suppressed M1 macrophage-associated signatures via CD47. (A) Thbs1 treatment reduced hepatic mRNA expression of the macrophage marker *Cd68* and M1 markers *Cd86* and *Nos2*; CD47 OE attenuated these effects; (B) Representative F4/80 immunohistochemistry (scale bar = 50 μm) and immunofluorescence staining (scale bar = 100 μm) of mouse liver sections. Images are provided as qualitative representations of hepatic macrophage infiltration; (C) *In vitro* experimental design to confirm that the effect of Thbs1 is related to the inhibition of M1 macrophage-associated signatures; (D and E) Effects of Thbs1 on M1/M2 markers and cytokines in LPS-stimulated RAW264.7 cells. RAW264.7 macrophages were stimulated with LPS (100 ng/mL) for 24 h in the presence or absence of Thbs1. For *in vivo* experiments, $n = 8$ mice per group were initially included; after outlier exclusion using ROUT ($Q = 5\%$), 6–8 samples per group were used for statistical analysis. *In vitro* experiments were independently repeated three times ($n = 3$). Data are presented as mean \pm SD. Statistical significance was determined using one-way ANOVA, with Tukey's multiple comparisons test for correction. $P < 0.05$ was considered statistically significant. ANOVA: Analysis of variance; CD47: cluster of differentiation 47; LPS: lipopolysaccharide; M1: classically activated macrophage phenotype; M2: alternatively activated macrophage phenotype; mRNA: messenger RNA; OE: overexpression; RAW264.7: murine macrophage cell line RAW264.7; ROUT: robust regression and outlier removal; SD: standard deviation; Thbs1: thrombospondin-1; *Cd68*: cluster of differentiation 68; *Cd86*: cluster of differentiation 86; *Nos2*: nitric oxide synthase 2; *Adgre1*: adhesion G protein-coupled receptor E1; *Arg1*: arginase 1; *Il1b*: interleukin-1 β ; *Il6*: interleukin-6; *Il23a*: interleukin-23 α ; *Ccl2*: C-C motif chemokine ligand 2; *Tnf*: tumor necrosis factor- α ; *Il10*: interleukin-10.

DISCUSSION

This study delineates a Thbs1-CD47 axis that links circulating indicator dynamics to macrophage-centered immunoregulation in MASH [Figure 5]. Clinically, circulating Thbs1 tracked disease activity, correlating positively with histological severity and declining after effective intervention. In a diet-induced MASH

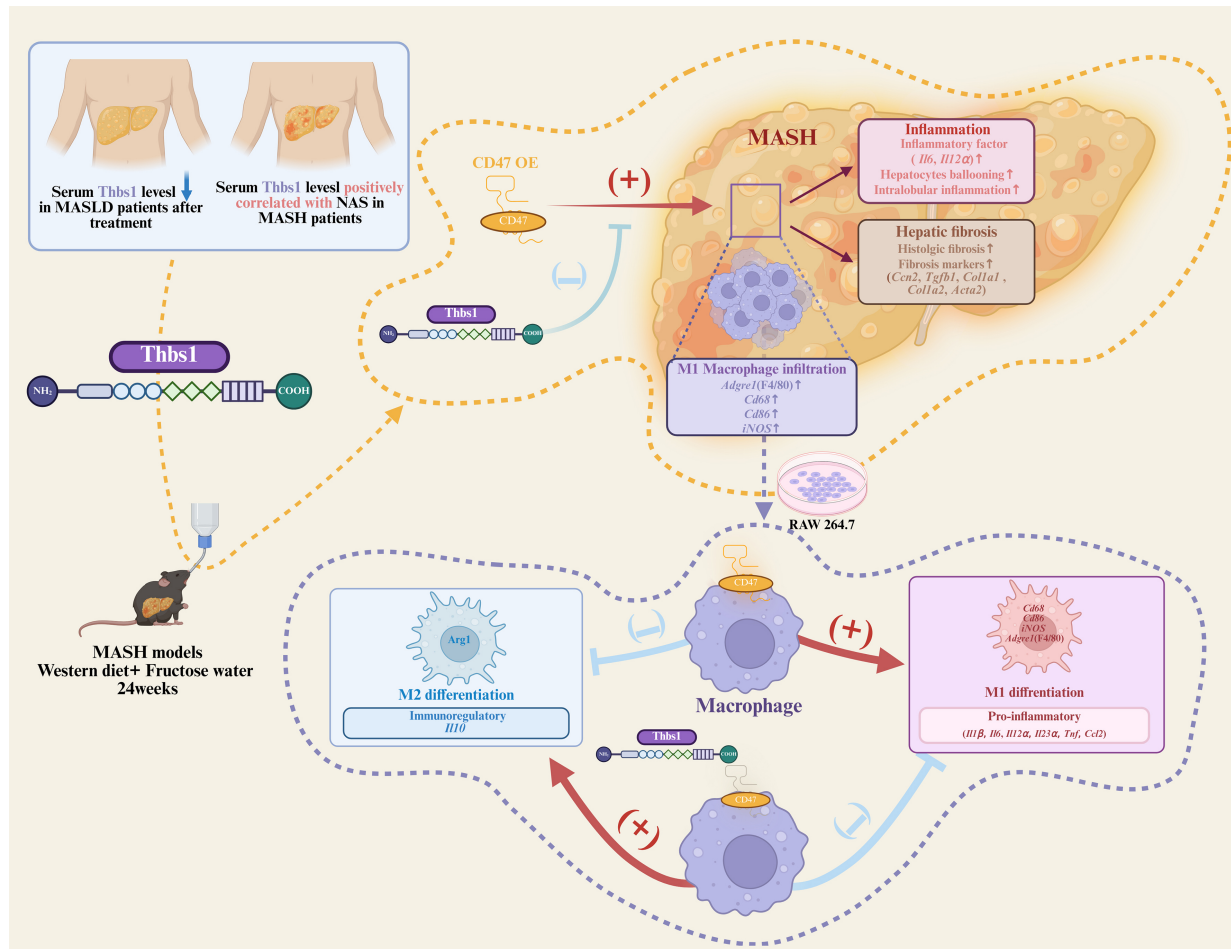


Figure 5. Thbs1 improves diet-induced MASH by regulating hepatic macrophage inflammatory responses through CD47. Clinically, serum Thbs1 tracks MASLD and MASH activity. In mice, Thbs1 limits hepatic macrophage infiltration and M1 macrophage-skewed programs, which are attenuated by liver-specific CD47 overexpression, thereby relieving hepatic inflammation and fibrosis. This figure was created using BioRender. Bian, C. (2026) <https://BioRender.com/jeldwz5>. CD47: cluster of differentiation 47; MASLD: metabolic dysfunction-associated steatotic liver disease; MASH: metabolic dysfunction-associated steatohepatitis; M1: classically activated macrophage phenotype; Thbs1: thrombospondin-1; Acta2: actin alpha 2 smooth muscle; Adgre1: adhesion G protein-coupled receptor E1; Ccl2: C-C motif chemokine ligand 2; Ccn2: cellular communication network factor 2; Cd68: cluster of differentiation 68; Cd86: cluster of differentiation 86; Col1a1: collagen type I alpha 1 chain; Col1a2: collagen type I alpha 2 chain; iNOS: inducible nitric oxide synthase; Il1 β : interleukin-1 β ; Il6: interleukin-6; Il10: interleukin-10; Il12 α : interleukin-12 α ; Il23 α : interleukin-23 α ; M2: alternatively activated macrophage phenotype; NAS: NAFLD Activity Score; Tgfb1: transforming growth factor- β 1; Tnf: tumor necrosis factor- α .

mouse model, short-term Thbs1 administration attenuated hepatic inflammation and fibrosis. Importantly, these benefits were related to CD47 signaling: Thbs1 reduced hepatic macrophage infiltration and M1 macrophage-associated inflammatory signatures *in vivo*, whereas liver-specific CD47 OE blunted these effects; *in vitro*, Thbs1 suppressed LPS-induced M1 macrophage-associated signatures and pro-inflammatory cytokine expression. Collectively, our findings support a model in which the Thbs1-driven inhibition of macrophage inflammation and fibrogenesis in MASH is attenuated by liver-specific CD47 OE.

Our results extend prior evidence that Thbs1 participates in metabolic and inflammatory regulation. Thbs1 is minimally expressed in healthy liver but is upregulated in fibrotic and cirrhotic conditions, including MASH-related cirrhosis, and has been linked to hepatic fat content in MASLD^[15]. The observation that serum Thbs1 decreases with clinical improvement while showing a modest positive association with histological severity in our biopsy-proven cohort supports its potential relevance as a circulating indicator of disease activity. Consistently, our multivariate regression analyses showed that Thbs1 maintained its

association with NAS after adjustment for key clinical covariates, including BMI, liver enzymes, and lipid profiles. Together, these findings suggest that circulating Thbs1 may reflect dynamic changes in disease activity and could serve as a complementary, non-invasive indicator for the clinical assessment of MASH. This observational pattern also provides a clinical context for interpreting the directionality of Thbs1-associated effects in experimental settings.

In this study, although circulating Thbs1 levels were positively associated with disease severity in patients, our experimental data showed that Thbs1 was associated with reduced inflammatory and fibrotic features in MASH models. This apparent discrepancy may reflect a compensatory upregulation of Thbs1 in response to hepatic injury and inflammation as part of an endogenous mechanism to modulate macrophage-driven inflammatory responses. In line with this possibility, Thbs1 has been implicated in the regulation of macrophage activation, efferocytosis, and inflammatory resolution, while its effects appear to be highly dependent on cellular source, disease stage, and tissue context^[4,16,17]. Thus, elevated circulating Thbs1 in patients may not necessarily indicate a direct pathogenic role, but could instead reflect a counter-regulatory or injury-responsive program activated during hepatic inflammation.

To further explore these associations under controlled conditions, we employed a diet-only MASH model (Western diet plus fructose water for 22 weeks) that reproduces key histological and metabolic features of human MASH, including steatosis, lobular inflammation, and early fibrosis^[18]. Compared with genetic or toxin-based models, diet-induced paradigms more closely mirror the natural history of MASLD/MASH in clinical settings^[19], thereby providing a relevant context to evaluate Thbs1 intervention and the contribution of CD47. In this experimental framework, the anti-inflammatory effects of Thbs1 aligned with its reported roles in immune modulation and inflammation resolution^[4]. Herein, Thbs1 reduced hepatic pro-inflammatory cytokine expression and attenuated lobular inflammation and early pro-fibrotic signaling, whereas steatosis and lipogenic protein abundance were not significantly altered over the 10-day course. This apparent dissociation is plausible given that short interventions often fail to reverse established hepatic lipid accumulation or body weight, which typically requires longer treatment durations to change^[20]. Therefore, while Thbs1 administration attenuated hepatic inflammatory and early pro-fibrotic features under the current experimental conditions, it is possible that the relatively short time (10 days) was insufficient to elicit detectable changes in steatosis. Moreover, stage-dependent remodeling of lipid metabolic programs during MASH progression, including “burn-out” steatosis in more advanced disease, may further limit detectable changes in steatosis over brief time frames^[21,22]. Therefore, longer-term studies are needed to determine whether Thbs1 also influences hepatic lipid metabolism.

To further examine the signaling context underlying these effects, CD47 was evaluated as a key receptor for Thbs1. CD47 has been implicated in redox balance and inflammatory stress signaling^[23]. Given this functional linkage, the Thbs1-CD47 interaction provides a relevant context for interpreting the downstream immunometabolic effects observed herein. Interestingly, we also observed that CD47 OE paradoxically reduced liver weight and insulin tolerance. This suggests a more complex, context-dependent role for CD47 beyond simple antagonism of Thbs1. As a pleiotropic receptor, CD47 may modulate systemic metabolic processes, lipid redistribution, or insulin signaling cascades under specific pathological contexts. Indeed, robust evidence from both genetic and pharmacological studies highlights the involvement of CD47 in metabolic regulation; specifically, genetic deficiency of CD47 protects mice from diet-induced obesity and improves insulin sensitivity^[24], and recent findings demonstrate that pharmacological blockade of CD47 confers profound metabolic benefits against obesity^[25].

Within this signaling context, prior mechanistic work suggests that CD47 signaling may interface with CD14-associated pathways involved in inflammatory responses. Stein *et al.* reported in an *in vitro* macrophage system that Thbs1 signaling via CD47 can restrain inflammatory priming by modulating

CD14-associated TLR signaling^[8]. Consistently, our *in vivo* data provide convergent evidence at the phenotypic and transcriptional levels: Thbs1 decreased hepatic inflammatory and fibrotic readouts, accompanied by reduced hepatic *CD14* mRNA, whereas hepatic CD47 OE reversed these changes. Together, these findings are consistent with the involvement of a Thbs1-CD47-CD14 signaling context, in which excess CD47 helps maintain a CD14-linked priming capacity in the liver microenvironment, thereby counteracting Thbs1-associated immunomodulatory effects in MASH.

In agreement with this signaling context, Thbs1 reduced hepatic macrophage infiltration and M1 macrophage-associated markers, and these effects were attenuated by CD47 OE. Given that macrophage recruitment and M1 macrophage-skewed programs promote MASH progression and fibrogenesis through cytokines, such as TGF β 1, that activate hepatic stellate cells^[26], our findings support a role for Thbs1 in modulating the inflammatory-fibrotic cascade in this signaling context. This interpretation is further supported by our RAW264.7 experiments, which showed that Thbs1 suppresses LPS-induced M1 macrophage markers and pro-inflammatory cytokines while increasing IL-10 expression.

Taken together, these findings suggest an association between Thbs1 and macrophage-related inflammatory responses in MASH, potentially within a CD47-linked signaling framework. This interpretation is consistent with the observed associations in patients and accommodates the context-dependent effects observed in experimental models. However, given the observational nature of the clinical analyses and the short-term experimental design, these findings should be interpreted with caution. Further studies are required to clarify the temporal dynamics, cell-specific mechanisms, and broader relevance of Thbs1-CD47-associated signaling in MASH progression.

Limitations

First, the clinical RCT data analyzed herein were not initially designed to assess Thbs1 as a direct intervention target. Therefore, the observed decrease in serum Thbs1 levels following treatment should be cautiously interpreted as an associative finding reflecting MASH improvement, rather than establishing a definitive causal relationship. Second, we primarily relied on a single diet-induced MASH model (Western diet plus fructose), which primarily reflects obese MASH. Lean MASH is another important clinical phenomenon; therefore, validation across complementary models representing distinct MASH phenotypes would strengthen the generalizability. Third, the 10-day Thbs1 regimen in our MASH mouse model is quite short. While this duration is sufficient for observing acute anti-inflammatory responses and downregulation of fibrotic markers, it is likely insufficient to fully reverse established hepatic fibrosis or significantly modify macroscopic steatosis phenotypes. A longer intervention study could provide more comprehensive insights into sustained intervention efficacy and additional metabolic effects. Fourth, CD47 is widely expressed in multiple hepatic cell types, including macrophages, hepatocytes, and endothelial cells. Here, the liver-targeted CD47 OE using adenoviral vectors likely affected hepatocytes predominantly, and thus did not allow discrimination of cell type-specific effects. Future studies using cell type-specific genetic approaches will be necessary to dissect the precise cellular mechanisms underlying the Thbs1-CD47 axis. Fifth, the macrophage inflammatory phenotype in this study was primarily evaluated using selected M1 macrophage-associated markers (e.g., CD86, NOS2) and inflammatory gene expression. While these are established approaches, they do not fully capture the dynamic nature of macrophage phenotypes, and therefore future studies incorporating comprehensive techniques, such as flow cytometry or single-cell transcriptomics, are warranted. Sixth, while our study demonstrates that CD47 OE reduces the modulatory effects of Thbs1 on M1 macrophage-associated signatures, the specific downstream molecular events following the Thbs1-CD47 interaction *in vivo* are inferred rather than directly measured. Precisely delineating these *in vivo* mechanistic links represents a critical objective for our future research. Finally, our mechanistic interpretation of the Thbs1-CD47 axis is based mainly on murine liver and macrophage systems; further validation in human MASH samples will be important for clinical translation.

Conclusion

Thbs1 suppresses M1 macrophage-associated signatures via CD47, thereby attenuating liver inflammation and early fibrotic features in MASH mice. These data highlight the Thbs1-CD47 axis as a potential stage-informed target for MASH treatment.

DECLARATIONS

Acknowledgments

We would like to express our gratitude to all patient participants in the study.

Authors' contributions

Conceptualization, funding acquisition, project administration, resources, supervision, writing, review, and editing: Bian H, Zhu X

Conceptualization, project administration, resources, supervision, writing, reviewing, and editing: Gao X

Formal analysis, investigation, validation, visualization, and writing of the original draft: Liu Q, Fan C, Xu B

Funding acquisition, formal analysis, and investigation: He Y

Formal analysis and investigation: Yang X, Zhang Y, Sun X, Li S, Zhang M, Ban X, Aikebaier G, Bai Z, Duan W, Yan H, Chang X, Xia M

All the authors have read and approved the final manuscript.

Availability of data and materials

The datasets used and/or analyzed during the current study are available from the corresponding author upon reasonable request.

AI and AI-assisted tools statement

During the preparation of this manuscript, the AI tool Nano Banana Pro (version Gemini 3 Pro Image, released 2025-11-20) was used solely to generate original schematic elements for [Figures 1, 3, and 4](#), and the Graphical Abstract. Adobe Illustrator (version 29.6.1) was used to arrange and finalize these elements. The tools did not influence the study design, data collection, analysis, interpretation, or the scientific content of the work. All authors take full responsibility for the accuracy, integrity, and final content of the manuscript.

Financial support and sponsorship

This study was supported by the National Key Research and Development Program of China (Grant No.2023ZD0508703 to Bian H), National Natural Science Foundation of China (Grant No.82370870 to Bian H, Grant No.82100849 to Zhu X, and Grant No.82100827 to He Y), Science and Technology Commission of Shanghai Municipality (Grant No.22Y31900302 to Bian H), Shanghai Municipal Health Commission (Grant No. 202240295 to Bian H), and the Young Foundation of Zhongshan Hospital Fudan University (Grant No.2023-006 to Zhu X).

Conflicts of interest

All authors declared that there are no conflicts of interest.

Ethics approval and consent to participate

This study was approved by the Ethics Committee of Zhongshan Hospital, Fudan University, China (Approval No. B2022-152). Written informed consent was obtained from all participants. All the procedures were performed in accordance with the principles of the Declaration of Helsinki. All animal experiments were conducted according to the protocols approved by the Department of Laboratory Animal Science, Fudan University (Approval No. 202111017S).

Consent for publication

Not applicable.

Copyright

© The Author(s) 2026.

Supplementary Materials

Supplementary Materials

REFERENCES

1. Rinella ME, Lazarus JV, Ratziu V, et al.; NAFLD Nomenclature consensus group. A multisociety Delphi consensus statement on new fatty liver disease nomenclature. *J Hepatol*. 2023;78:1966-86. [DOI PubMed PMC](#)
2. Targher G, Byrne CD, Tilg H. MASLD: a systemic metabolic disorder with cardiovascular and malignant complications. *Gut*. 2024;73:691-702. [DOI PubMed](#)
3. Kasper P, Martin A, Lang S, et al. NAFLD and cardiovascular diseases: a clinical review. *Clin Res Cardiol*. 2021;110:921-37. [DOI PubMed PMC](#)
4. Kaur S, Roberts DD. Emerging functions of thrombospondin-1 in immunity. *Semin Cell Dev Biol*. 2024;155:22-31. [DOI PubMed PMC](#)
5. Li Y, Turpin CP, Wang S. Role of thrombospondin 1 in liver diseases. *Hepatol Res*. 2017;47:186-93. [DOI PubMed PMC](#)
6. Matsuo Y, Tanaka M, Yamakage H, et al. Thrombospondin 1 as a novel biological marker of obesity and metabolic syndrome. *Metabolism*. 2015;64:1490-9. [DOI PubMed PMC](#)
7. Bai J, Xia M, Xue Y, et al. Thrombospondin 1 improves hepatic steatosis in diet-induced insulin-resistant mice and is associated with hepatic fat content in humans. *EBioMedicine*. 2020;57:102849. [DOI PubMed PMC](#)
8. Stein EV, Miller TW, Ivins-O'Keefe K, Kaur S, Roberts DD. Secreted thrombospondin-1 regulates macrophage interleukin-1 β production and activation through CD47. *Sci Rep*. 2016;6:19684. [DOI PubMed PMC](#)
9. Yan HM, Xia MF, Wang Y, et al. Efficacy of berberine in patients with non-alcoholic fatty liver disease. *PLoS One*. 2015;10:e0134172. [DOI PubMed PMC](#)
10. Rinella ME, Neuschwander-Tetri BA, Siddiqui MS, et al. AASLD Practice Guidance on the clinical assessment and management of nonalcoholic fatty liver disease. *Hepatology*. 2023;77:1797-835. [DOI PubMed PMC](#)
11. European Association for the Study of the Liver (EASL), European Association for the Study of Diabetes (EASD), European Association for the Study of Obesity (EASO). EASL-EASD-EASO Clinical Practice Guidelines on the management of metabolic dysfunction-associated steatotic liver disease (MASLD). *J Hepatol*. 2024;81:492-542. [DOI PubMed](#)
12. Chen S, Lu Z, Jia H, et al. Hepatocyte-specific Mas activation enhances lipophagy and fatty acid oxidation to protect against acetaminophen-induced hepatotoxicity in mice. *J Hepatol*. 2023;78:543-57. [DOI PubMed](#)
13. Wu K, Yuan Y, Yu H, et al. The gut microbial metabolite trimethylamine N-oxide aggravates GVHD by inducing M1 macrophage polarization in mice. *Blood*. 2020;136:501-15. [DOI PubMed PMC](#)
14. Liu W, You D, Lin J, et al. SGLT2 inhibitor promotes ketogenesis to improve MASH by suppressing CD8⁺ T cell activation. *Cell Metab*. 2024;36:2245-61.e6. [DOI PubMed](#)
15. Murphy-Ullrich JE, Suto MJ. Thrombospondin-1 regulation of latent TGF- β activation: a therapeutic target for fibrotic disease. *Matrix Biol*. 2018;68-69:28-43. [DOI PubMed PMC](#)
16. Kale A, Rogers NM, Ghimire K. Thrombospondin-1 CD47 signalling: from mechanisms to medicine. *Int J Mol Sci*. 2021;22:4062. [DOI PubMed PMC](#)
17. Gwag T, Reddy Mooli RG, Li D, Lee S, Lee EY, Wang S. Macrophage-derived thrombospondin 1 promotes obesity-associated non-alcoholic fatty liver disease. *JHEP Rep*. 2021;3:100193. [DOI PubMed PMC](#)
18. Boland ML, Oró D, Tølbøl KS, et al. Towards a standard diet-induced and biopsy-confirmed mouse model of non-alcoholic steatohepatitis: Impact of dietary fat source. *World J Gastroenterol*. 2019;25:4904-20. [DOI PubMed PMC](#)
19. Gallage S, Avila JEB, Ramadori P, et al. A researcher's guide to preclinical mouse NASH models. *Nat Metab*. 2022;4:1632-49. [DOI PubMed](#)
20. Tamaki N, Ajmera V, Loomba R. Non-invasive methods for imaging hepatic steatosis and their clinical importance in NAFLD. *Nat Rev Endocrinol*. 2022;18:55-66. [DOI PubMed PMC](#)
21. Zhao L, Zhang C, Luo X, et al. CD36 palmitoylation disrupts free fatty acid metabolism and promotes tissue inflammation in non-alcoholic steatohepatitis. *J Hepatol*. 2018;69:705-17. [DOI PubMed](#)
22. Lian S, Lu M, Jiajing L, et al. Conjugated lithocholic acid activates hepatic TGR5 to promote lipotoxicity and MASLD-MASH transition by disrupting carnitine biosynthesis. *Adv Sci*. 2025;12:e2410602. [DOI PubMed PMC](#)
23. Dou M, Chen Y, Hu J, Ma D, Xing Y. Recent advancements in CD47 signal transduction pathways involved in vascular diseases. *Biomed Res Int*. 2020;2020:4749135. [DOI PubMed PMC](#)
24. Maimaitiyiming H, Norman H, Zhou Q, Wang S. CD47 deficiency protects mice from diet-induced obesity and improves whole body glucose tolerance and insulin sensitivity. *Sci Rep*. 2015;5:8846. [DOI PubMed PMC](#)

-
25. Su Y, Sun J, Li X, et al. CD47-blocking antibody confers metabolic benefits against obesity. *Cell Rep Med*. 2025;6:102089. DOI [PubMed](#) [PMC](#)
 26. Tsuchida T, Friedman SL. Mechanisms of hepatic stellate cell activation. *Nat Rev Gastroenterol Hepatol*. 2017;14:397-411. DOI [PubMed](#)

Disclaimer/Publisher's Note: All statements, opinions, and data contained in this publication are solely those of the individual author(s) and contributor(s) and do not necessarily reflect those of OAE and/or the editor(s). OAE and/or the editor(s) disclaim any responsibility for harm to persons or property resulting from the use of any ideas, methods, instructions, or products mentioned in the content.



© The Author(s) 2026. Open Access This article is licensed under a Creative Commons Attribution 4.0 International License (<https://creativecommons.org/licenses/by/4.0/>), which permits unrestricted use, sharing, adaptation, distribution and reproduction in any medium or format, for any purpose, even commercially, as long as you give appropriate credit to the original author(s) and the source, provide a link to the Creative Commons license, and indicate if changes were made.